K. Baganas, Ath. Kehagias and A. Charalambopoulos.
"Inhomogenous Dielectric Media: Wave Propagation and Dielectric Permittivity Reconstruction".

This paper has appeared in the journal:
Journal of Electromagnetic Waves and Applications, vol. 15, pp. 1373--1400, 2001.

Inhomogeneous Dielectric Media:

Wave Propagation and

Dielectric Permittivity Reconstruction

K. Baganas A. Kehagias A. Charalambopoulos

October 11, 2001

Department of Mathematics, Physical and Computational Sciences

School of Engineering, Aristotle University of Thessaloniki

GR54006 Thessaloniki, GREECE

Corresponding Author:

Antonios Charalambopoulos

Department of Mathematics, Physical and Computational Sciences

School of Engineering, Aristotle University of Thessaloniki

GR 54006 Thessaloniki, GREECE

Short Title: Wave Propagation and Dielectric Permittivity Reconstruction

Abstract

In this paper we study the propagation of electromagnetic waves in a waveguide completely filled with a inhomogeneous dielectric material. The material is inhomogeneous in the longitudinal direction, i.e. the dielectric permittivity is described by a function $\varepsilon = \varepsilon_0 \varepsilon_r(z)$. We first solve the direct problem; then we develop a computational procedure for solving the inverse problem and apply the procedure to the estimation of an unknown dielectric permittivity profile. An important feature of our approach is the expansion of the unknown $\varepsilon_r(z)$ into a power series. The dielectric permittivity profile estimation consists in determining the unknown coefficients through error function minimization. We test our method by numerical experiments utilizing a genetic algorithm and obtain very accurate results.

1 Introduction

In this paper we describe a method for estimating the dielectric permittivity profile of a material, inside a waveguide, which is axisymmetric and inhomogeneous along its axis. This requires the development of a novel method for the solution of electromagnetic wave propagation problems.

Maxwell's equations for electromagnetic wave propagation in isotropic and inhomogeneous media are PDE's with variable coefficients. Closed form solutions of these equations are available only for special cases of inhomogeneous profiles [1]. Approximate solutions can be obtained by replacing the actual medium with a finely layered one, where each layer is assumed to have constant permittivity [2, 3, 4, 5]. If these layers are much thinner than the wavelength of the propagation wave then sufficiently accurate solutions can be obtained. This approach is used by finite difference methods [6], the Transmission Line method [7], the WKB method together with asymptotic matching [2, 8], the propagation/scattering matrix method [2] etc.

In this work we propose an alternative technique which can be applied to dielectric profiles of the form $\varepsilon(z) = \epsilon_0 \varepsilon_r(z)$, where ϵ_0 is the dielectric permittivity in the free space and $\varepsilon_r(z)$ is the relative dielectric permittivity. Our technique requires only that $\varepsilon_r(z)$ can be expanded in a *power series*.

Applying separation of variables in cylindrical coordinates to the field equations results, for the z-dependent part of the electric field, in an ODE with nonconstant coefficients. Motivated by the expansion of $\varepsilon_r(z)$ in power series we solve the aforementioned ODE by the *Frobenius* method. This results in recursive equations for the expansion coefficients of the electric field. These equations can be solved symbolically or numerically.

We have applied the above technique to the direct, as well as to the inverse propagation problem, in a cylindrical waveguide series consisting of three parts: a central inhomogeneous waveguide and two lateral homogeneous ones. The solution of the direct problem provides the necessary background for the dielectric profile reconstruction which constitutes the inverse problem. For the complete solution

of the inverse problem we utilize an error function minimization approach which makes use of a genetic algorithm; the minimizing solution consists of the coefficients ε_0, ε_1, ε_2... in the expansion of $\varepsilon_r(z)$. We have used third order expansions but the method can be easily generalized. We have applied this method to the estimation of specific dielectric permittivity profiles and obtained very accurate estimates.

2 Maxwell's Equations in Inhomogeneous Media

For a continuous longitudinally inhomogeneous dielectric material with dielectric permittivity $\varepsilon(z) = \epsilon_0\varepsilon_r(z)$, Maxwell's equations yield the following equations, which characterize the phasor $\mathbf{E}(\mathbf{r})$ of the time harmonic electric field

$$\nabla \cdot (\varepsilon_r(z)\mathbf{E}) = 0 \tag{1}$$

$$\nabla(\nabla \cdot \mathbf{E}) - \nabla^2\mathbf{E} = k^2\varepsilon_r(z)\mathbf{E} \tag{2}$$

where $k = \omega\sqrt{\mu_0\epsilon_0}$ is the wavenumber, while $\omega = 2\pi f$ is the angular frequency and μ_0 is the magnetic permeability in free space.

We are interested in TE modes, expressed in cylindrical coordinates r, ϕ, z, in the form

$$\mathbf{E}(r, \phi, z) = E_r(r,\, \phi,\, z)\hat{\mathbf{r}} + E_\phi(r,\, \phi,\, z)\hat{\boldsymbol{\phi}} \tag{3}$$

where $\hat{\mathbf{r}}$, $\hat{\boldsymbol{\phi}}$ are the unit vectors in the radial-(r) and azimuthal-(ϕ) direction, respectively. Applying the separation of variables the components of the electric field become

$$E_r(r, \phi, z) = R_r(r)\,\Phi_r(\phi)\,Z_r(z)\,, \quad E_\phi(r, \phi, z) = R_\phi(r)\,\Phi_\phi(\phi)\,Z_\phi(z)\,.$$

Inserting these expressions in eq.(1), we obtain that

$$\frac{R_r'}{R_r} = -\frac{1}{r} - \frac{1}{r}\frac{R_\phi}{R_r}\frac{\Phi_\phi'}{\Phi_r}\frac{Z_\phi}{Z_r} \tag{4}$$

where R_r' denotes the first derivative of $R_r(r)$ function. Moreover, after some manipulations, eq.(2) results in the following equations

$$\frac{R_r''}{R_r} + \frac{1}{r}\frac{R_r'}{R_r} + \frac{1}{r^2}\frac{\Phi_r''}{\Phi_r} + \frac{Z_r''}{Z_r} - \frac{1}{r^2} - \frac{2}{r^2}\frac{R_\phi \Phi_\phi' Z_\phi}{R_r \Phi_r Z_r} + k^2\varepsilon_r(z) = 0 \tag{5}$$

and

$$\frac{R_\phi''}{R_\phi} + \frac{1}{r}\frac{R_\phi'}{R_\phi} + \frac{1}{r^2}\frac{\Phi_\phi''}{\Phi_\phi} + \frac{Z_\phi''}{Z_\phi} - \frac{1}{r^2} + \frac{2}{r^2}\frac{R_r \Phi_r' Z_r}{R_\phi \Phi_\phi Z_\phi} + k^2\varepsilon_r(z) = 0\,. \tag{6}$$

Handling eq.(5) first, we apply standard separation of variable arguments leading to the relations

$$\frac{\Phi_\phi'}{\Phi_r} = \lambda\,, \quad (\lambda \text{ constant}) \tag{7}$$

$$\frac{Z_\phi}{Z_r} = q\,, \quad (q \text{ constant}) \tag{8}$$

as well as to the equations

$$\Phi_r'' - \mu\Phi_r = \Phi_r'' + n^2\Phi_r = 0\,, \quad n = 0, 1, 2, ... \tag{9}$$

$$Z_r'' + \left[k^2\varepsilon_r(z) - \xi^2\right] Z_r = 0 \tag{10}$$

$$r^2 R_r'' + r R_r' + [\mu + r^2\xi^2 - 1]R_r - 2\lambda q R_\phi = 0, \tag{11}$$

where μ, ξ are separation of variables constants. Notice that the only acceptable values of the constant

μ are $\mu = -n^2,\ n = 0, 1, 2, ...$, in order to obtain periodic solutions with period 2π. The special case $\mu = n = 0$ will be considered later in greater detail.

Thus, eq.(4) is written as

$$\frac{R_r'}{R_r} = -\frac{1}{r} - \frac{1}{r}\frac{R_\phi}{R_r}\lambda q \tag{12}$$

and combined with eq.(11) gives the following differential equation concerning $R_r(r)$

$$r^2 R_r'' + 3r R_r' + (r^2\xi^2 + \mu + 1)R_r = 0\,. \tag{13}$$

The general solution of eq.(13) is

$$R_r(r) = A_n r^{-1} J_n(\xi r) + B_n r^{-1} Y_n(\xi r) \tag{14}$$

(with arbitrary constants A_n, B_n) where J_n and Y_n are the Bessel functions of first and second kind, respectively. Once the radial function $R_r(r)$ is determined, then $R_\phi\,(r)$ can be determined through eq.(12) leading to the result

$$R_\phi(r) = -\frac{\xi}{q\lambda}[A_n J_n'(\xi r) + B_n Y_n'(\xi r)]\,. \tag{15}$$

In addition, eq.(9) gives immediately that

$$\Phi_r(\phi) = C_n \cos(n\phi) + D_n \sin(n\phi) \tag{16}$$

where C_n, D_n are constants. Using eq.(7) we infer that

$$\Phi_\phi(\phi) = \frac{\lambda}{n}[C_n \sin(n\phi) - D_n \cos(n\phi)] \tag{17}$$

where no integration constant is allowed since otherwise the separability of eq.(6) would be violated. In addition, note that eq.(6) is expected to separate variables if $\frac{\Phi''_\phi}{\Phi_\phi}$ is constant and this is guaranteed by eq.(17).

Let us now turn to the solution of eq.(11) and verify that the already constructed solution patches satisfy as well the relation (6), which originates from Maxwell's equations. Postponing the treatment of eq.(11), we exploit eqs.(7-10), (16), (17) and we see that eq.(6) can be rewritten as

$$r^2 R''_\phi + r R'_\phi + (r^2\xi^2 + \mu - 1)R_\phi + 2\frac{\mu}{\lambda q} R_r = 0\,. \tag{18}$$

So it must be shown that the general solution (15) satisfies as well eq.(18). This is accomplished if we replace the expressions (14), (15) in eq.(18) to obtain that

$$A_n \left[x^3 J'''_n(x) + x^2 J''_n(x) + \left(\mu + x^2 - 1\right) x J'_n(x) - 2\mu J_n(x)\right] +$$

$$B_n \left[x^3 Y'''_n(x) + x^2 Y''_n(x) + \left(\mu + x^2 - 1\right) x Y'_n(x) - 2\mu Y_n(x)\right] = 0 \tag{19}$$

where $x = \xi r$.

However, every term of the above equation vanishes separately, rendering eq.(19) and consequently eq.(18) valid. This is proven if we start with the Bessel equation

$$x^2 J''_n(x) + x J'_n(x) + (x^2 + \mu) J_n(x) = 0,$$

differentiate with respect to x and exploit again the validity of the Bessel equation. (Similar results hold for the term reffering to $Y_n(x)$.)

Let us now handle eq.(10). The relative dielectric permittivity has a power series expansion of the form

$$\varepsilon_r(z) = \sum_{i=0}^{\infty} \varepsilon_i z^i = \varepsilon_0 + \varepsilon_1 z + \varepsilon_2 z^2 + \dots . \tag{20}$$

We now use Frobenius method for solving eq.(10) and assume that $Z_r(z)$, the solution to this equation, can be expressed as

$$Z_r(z) = \sum_{i=0}^{\infty} c_i z^i = c_0 + c_1 z + c_2 z^2 + \dots \tag{21}$$

given that the center of expansion 0 is a regular point for the ODE (10) [9, 10]. Hence $Z_r(z)$ is determined by the coefficients c_i, $i = 0, 1, 2, \dots$. From now on our analysis will focus on determining these coefficients.

Substituting the expressions (20), (21) in eq.(10), we produce the following recursive scheme

$$(i+2)(i+1)c_{i+2} - \xi^2 c_i + k^2 \sum_{j=0}^{i} c_{i-j}\varepsilon_j = 0 \ , \quad i = 0, 1, 2, \dots .$$

Equivalently, setting $H^2 = k^2\varepsilon_0 - \xi^2$ we have

$$c_2 = -\frac{H^2}{2} c_0 \quad \text{and} \quad (i+2)(i+1)c_{i+2} + H^2 c_i + k^2 \sum_{j=1}^{i} c_{i-j}\varepsilon_j = 0 \ , \quad i = 1, 2, \dots . \tag{22}$$

From this scheme we infer that c_i ($i \geq 2$) are functions of c_0, c_1, H, k and the permittivity coefficients

ε_j, $j = 0, .., i-2$, i.e. $c_i = c_i(c_0,\, c_1,\, H,\, k,\, \varepsilon_0, .., \varepsilon_{i-2})$. More accurately, c_i can be written as:

$$c_i = c_0 u_i(H,\, k,\, \varepsilon_0, .., \varepsilon_{i-2}) \;+\; c_1 w_i(H,\, k,\, \varepsilon_0, .., \varepsilon_{i-2})$$

where u_i, w_i are smooth functions of their arguments. Actually, u_i, w_i generate two independent solutions of the second degree ODE (10) and c_0, c_1 are mixture coefficients.

Once the recursive equations (22) are solved, the sought "axial" parts $Z_r(z)$, $Z_\phi(z)$ of the electric fields are determined through their power series coefficients. All the other components of the fields have been already determined and so the solution of the equations (22) leads immediately to the solution of Maxwell's equations for the specific structure under consideration. The behavior of c_2, $c_3, ..,$ c_L can be studied analytically for small values of L; larger values of L require the use of a symbolic algebra package, e.g. *Maple*.

Any arbitrary coefficients appearing in the above solutions will be specified by boundary independent conditions pertaining to a specific problem.

Before proceeding further, let us mention that there exist two special cases concerning the values of the separation of variables constants μ and ξ not discussed before.

1. When $\mu = 0$, the variable ξ necessarily vanishes and we obtain the expressions $R_r = \frac{d_1}{r}$ and $R_\phi = d_2 r + \frac{d_3}{r}$ (d_1, d_2, d_3 constants).

2. When $\mu = -n^2 \neq 0$ and $\xi = 0$, the field expressions can be obtained from the general case taking the limit $\xi \to 0$ and exploiting the asymptotic behavior of the underlying functions.

3 Wave Propagation in a Cylindrical Waveguide

Let us apply the solutions presented in the previous section to the determination of the electromagnetic field in a cylindrical waveguide filled with a linear, isotropic, inhomogeneous and lossless dielectric

material. This implies that $\varepsilon_r(z)$ is a real valued function ($\mathrm{Im}\{\varepsilon_r(z)\} = 0$) [2].

We now exploit the boundary conditions for such a cylindrical waveguide. The remarks and expressions presented below apply to the case of $\varepsilon(r,\, \phi,\, z) = \epsilon_0 \varepsilon_r(z)$, as well as to the special case of constant dielectric permittivity. The following conditions must be satisfied by the TE electric field.

Condition 1: The electric field components must have bounded values at the center ($r = 0$) of the waveguide.

Condition 2: The tangential component must vanish on the cylindrical surface (i.e. at $r = a$, where a is the waveguide radius) of the waveguides, i.e. $E_\phi(\alpha,\, \phi,\, z) = 0$ for $\phi \in [0, 2\pi]$.

Let us examine the general solution for $\mu = -n^2$, $n = 1, 2, ..$, in light of the above conditions.

From Condition 1 it follows that solutions which include Bessel's functions of second kind and their derivatives are rejected because of their singularities at $r = 0$. This can be seen from their behavior as $x \to 0$:

$$Y_n(x) = \begin{cases} -\frac{\Gamma(n)}{\pi}(\frac{2}{x}) + O(x \ln(x)) \ , & n = 1 \\ -\frac{\Gamma(n)}{\pi}(\frac{2}{x})^n + O(x^{2-n}) \ , & n \geq 2 \end{cases}$$

where $\Gamma(n)$ is the Gamma function. Bessel's functions of first kind have the following asymptotic behavior as $x \to 0$:

$$J_n(x) = \frac{1}{\Gamma(n+1)}(\frac{x}{2})^n + O\left(x^{n+2}\right) \ , \quad n = 1, 2...$$

and so they are acceptable as part of the solution. In conclusion, the solution will consist of combinations of terms of the form $\frac{J_n(x)}{x}$ and $J_n'(x)$, which vanish as $x \to 0$.

From Condition 2 we infer that $J_n'(\xi a) = 0$, from which results the discretization of the ξ, i.e. ξ can only take the values $\xi_{nm} = \frac{x_{nm}}{a}$, where x_{nm} is the m-th root of $J_n'(x)$ and $m = 1, 2, \ldots$. Discreteness of

ξ implies that H also takes discrete values, namely $H = H_{nm} = \sqrt{k^2\varepsilon_0 - \xi_{nm}^2}$. Hence, we obtain the TE field expressions inside the waveguide, which are

$$R_r(r) = A_n \frac{J_n(\xi_{nm} r)}{r} \ , \quad R_\phi(r) = -\frac{\xi_{nm}}{\lambda q} A_n J_n'(\xi_{nm} r) \ , \quad n, m = 1, 2, ...$$

$$\Phi_r(\phi) = C_n \cos(n\phi) + D_n \sin(n\phi) \ , \quad \Phi_\phi(\phi) = \frac{\lambda}{n}[C_n \sin(n\phi) - D_n \cos(n\phi)] \ , \quad n = 1, 2, ...$$

$$Z_r(z) = \sum_{i=0}^{\infty} c_i z^i = c_0 + c_1 z + c_2 z^2 + ... \ , \quad Z_\phi(z) = q Z_r(z) \tag{23}$$

where for every choice n, $m = 1, 2, ...$ the c_i's satisfy the recursive equation:

$$c_2 = -\frac{H_{nm}^2}{2} c_0 \ , \quad (i+2)(i+1)c_{i+2} + H_{nm}^2 c_i + k^2 \sum_{j=1}^{i} c_{i-j}\varepsilon_j = 0 \ , \quad i = 1, 2, \ldots . \tag{24}$$

In the case of constant dielectric permittivity, the z dependence of the field is trigonometric, as can be deduced easily from eq.(10); eqs.(23), (24) will be used in the case of non-constant dielectric permittivity.

Concerning the special case $\mu = 0$, Condition 1 implies that the R_r component and the d_3 coefficient of the R_ϕ component must vanish. Also, Condition 2 implies that $d_2 = 0$ or $E_\phi = 0$. Thus, azimuthally symmetric solutions cannot exist.

4 The Direct Problem for a System of Cylindrical Waveguides

Estimating the dielectric permittivity requires solving a direct problem for a *measurement device*. In this section we present the particular device under investigation and solve the corresponding direct problem.

4.1 The Measurement Device

The measurement device consists of three cylindrical waveguides interconnected in the manner illustrated in Figure 1.

Figure 1 to be placed here.

The left and the right waveguide have constant relative dielectric permittivity ε_c. The middle waveguide contains the inhomogeneous dielectric material. This will be the target of our investigation of the inverse problem . These waveguides are being excited by appropriate TE electric modes generated by a signal source. We assume perfect interconnection between the waveguides, a load adapted to the end of the right waveguide (which results in perfect/ideal absoption of the incident field at that point) and two measurement probes which cause negligible field distortion.

We now perform the field analysis of this system; in particular we study the propagation of the TE_{11} mode, which is the main mode for cylindrical waveguides. We also introduce a simplification for the remainder of the analysis. Up to this point we have assumed the relative dielectric permittivity to be given by a Taylor series expansion of the form

$$\varepsilon_r(z) = \varepsilon_0 + \varepsilon_1 z + \varepsilon_2 z^2 + \dots .$$

Of course, for all practical purposes, such an expansion will terminate after a finite number of terms. From now on, we specifically assume that $\varepsilon_r(z)$ is a third order polynomial, i.e. that

$$\varepsilon_r(z) = \varepsilon_0 + \varepsilon_1 z + \varepsilon_2 z^2 + \varepsilon_3 z^3 .$$

We have found a third order polynomial to be sufficient for quite accurate approximation of slowly varying smooth profile functions. Of course, the following analysis can be generalized to N-th order polynomials of the form $\varepsilon_r(z) = \varepsilon_0 + \varepsilon_1 z + ... + \varepsilon_N z^N$.

4.2 Computation of the Field Components

Let us first consider the frequencies at which field propagation occurs.

The cut-off frequencies in the two lateral waveguides, which have relative permittivity $\varepsilon_r = \varepsilon_c$, are the following [11]

$$\mathbf{f}_{c,nm} = \frac{\xi_{nm}}{2\pi\sqrt{m_0 e_0 \varepsilon_c}}\,, \quad n, m = 1, 2, \ldots .$$

Examining the propagation of TE_{1m} modes we restrict the above cut-off frequencies as follows

$$\mathbf{f}_{c,1m} = \frac{\xi_{1m}}{2\pi\sqrt{m_0 e_0 \varepsilon_c}}\,, \quad m = 1, 2, \ldots .$$

This implies that the excitation frequency f must be greater than the first cut-off frequency $\mathbf{f}_{c,11}$ which takes the form

$$\mathbf{f}_{c,11} = \frac{\xi_{11}}{2\pi\sqrt{m_0 e_0 \varepsilon_c}} = \frac{1.841}{2\pi a\sqrt{m_0 e_0 \varepsilon_c}}\,.$$

Hence the use of excitation frequency $f > \mathbf{f}_{c,11}$ is a prerequisite for the trasmission of a wave through the system of the three waveguides. Consider for a moment the case when the central waveguide is filled with a material of constant dielectric permittivity. In this case, if f is higher than $\mathbf{f}_{c,11}$ and lower than $\mathbf{f}_{c,12}$ it can be expected that the wave will propagate through the entire system in TE_{11} mode only. A similar argument can be applied when the central waveguide is filled with a material of variable

dielectric permittivity. This claim will be justified in Section 4.4. At this point we simply note that by judicious choice of the excitation frequency, it will be sufficient to compute the TE_{11} field expressions inside the three waveguides. In what follows ε_c is the constant relative permittivity of the left or the right waveguide, $\beta = \sqrt{k^2\varepsilon_c - \xi_{11}^2}$, $k = \omega\sqrt{\mu_0\epsilon_0}$ and $\xi_{11} = \frac{x_{11}}{a} = \frac{1.841}{a}$.

Waveguide no.1: The field expressions are

$$E_r(r,\, \phi,\, z) = \frac{j\omega\mu_0}{\xi_{11}^2} C \frac{J_1(\xi_{11} r)}{r} \sin(\phi)(e^{-j\beta z} + Ge^{j\beta z})$$

$$E_\phi(r,\, \phi,\, z) = \frac{j\omega\mu_0}{\xi_{11}} C J_1'(\xi_{11} r) \cos(\phi)(e^{-j\beta z} + Ge^{j\beta z})$$

where C is an arbitrary amplitude constant and G is the *reflection coefficient*.

Waveguide no.2: The field expressions are

$$E_r(r,\, \phi,\, z) = \frac{j\omega\mu_0}{\xi_{11}^2} C \frac{J_1(\xi_{11} r)}{r} \sin(\phi) \sum_{i=0}^{\infty} c_i z_i \,, \quad E_\phi(r,\, \phi,\, z) = \frac{j\omega\mu_0}{\xi_{11}} C J_1'(\xi_{11} r) \cos(\phi) \sum_{i=0}^{\infty} c_i z_i \,.$$

Waveguide no.3: The field expressions are

$$E_r(r,\, \phi,\, z) = \frac{j\omega\mu_0}{\xi_{11}^2} CD \frac{J_1(\xi_{11} r)}{r} \sin(\phi) e^{-j\beta z} \,, \quad E_\phi(r,\, \phi,\, z) = \frac{j\omega\mu_0}{\xi_{11}} CD J_1'(\xi_{11} r) \cos(\phi) e^{-j\beta z},$$

where D is the *transmission coefficient*.

Let us set $\boldsymbol{\varepsilon} = [\varepsilon_0\ \varepsilon_1\ \varepsilon_2\ \varepsilon_3]$. Recall that in the framework of the inverse problem the quantities obtained by the measurement device will be $D = D(\boldsymbol{\varepsilon},\, f,\, a,\, d)$, $G = G(\boldsymbol{\varepsilon},\, f,\, a,\, d)$, where f, a, d will be known for a particular experiment, while $\boldsymbol{\varepsilon}$ will be the quantity we want to determine. On the one hand, D, G can be measured; on the other hand, we will now determine their functional dependence on ε_0, ε_1, ε_2, ε_3 (and f, a, d); our final task will be to determine appropriate values for ε_0, ε_1, ε_2, ε_3 such that the theoretically computed D, G measurements agree with the ones obtained from field

measurements.

Hence our next task is to obtain concrete functional expressions $D(\boldsymbol{\varepsilon},\, f,\, a,\, d)$ and $G(\boldsymbol{\varepsilon},\, f,\, a,\, d)$. To this end we use the impendance conditions for the three waveguides.

At the interface $z = 0$, from the continuity of the components and their derivatives, we have that

$$c_0 = 1 + G \tag{25}$$

$$c_1 = -j\beta \cdot (1 - G)\,. \tag{26}$$

Similarly, at the interface $z = d$ the continuity of the components and their derivatives leads to

$$\sum_{i=0}^{\infty} c_i d^i = De^{-j\beta d} \Leftrightarrow c_0 Z_1(d) + c_1 Z_2(d) = De^{-j\beta d} \tag{27}$$

$$\sum_{i=1}^{\infty} i c_i d^{i-1} = -j\beta De^{-j\beta d} \Leftrightarrow c_0 Z_1'(d) + c_1 Z_2'(d) = -j\beta De^{-j\beta d} \tag{28}$$

where $Z_1(d) = 1 + u_2 d^2 + u_3 d^3 + ...$ and $Z_2(d) = d + w_2 d^2 + w_3 d^3 + ...\,.$

Eqs.(25-28) can be written as a 4x4 linear system: $AX = B$, where

$$A = \begin{bmatrix} 1 & 0 & -1 & 0 \\ 0 & 1 & -j\beta & 0 \\ Z_1(d) & Z_2(d) & 0 & -e^{-j\beta d} \\ Z_1'(d) & Z_2'(d) & 0 & j\beta e^{-j\beta d} \end{bmatrix}, \quad X = \begin{bmatrix} c_0 \\ c_1 \\ G \\ D \end{bmatrix}, \quad B = \begin{bmatrix} 1 \\ -j\beta \\ 0 \\ 0 \end{bmatrix}.$$

Hence A and B are completely specified in terms of known parameters, X contains the unknowns of the direct problem and $AX = B$ is a linear matrix equation which can be solved analytically by matrix inversion. Solving $AX = B$ with *Maple* is quite straightforward and yields the required expressions $D(\boldsymbol{\varepsilon},\, f,\, a,\, d)$ and $G(\boldsymbol{\varepsilon},\, f,\, a,\, d)$; these are not presented here for economy of space.

4.3 Agreement with Existing Solutions

We will now test the agreement of our solution with already existing analytical solutions for two simple dielectric profiles.

Case 1: $\varepsilon_r(z) \equiv \varepsilon_m =$ constant. In this case the field expressions inside the medium waveguide become

$$E_r(r,\, \phi,\, z) = \frac{j\omega\mu_0}{\xi_{11}^2} \cdot C \frac{J_1(\xi_{11} r)}{r} \sin(\phi)(C_m e^{-j\beta_m z} + G_m e^{j\beta_m z}),$$

$$E_\phi(r,\, \phi,\, z) = \frac{j\omega\mu_0}{\xi_{11}} C J_1'(\xi_{11} r) \cos(\phi)(C_m e^{-j\beta_m z} + G_m e^{j\beta_m z})$$

where m denotes the medium waveguide, C_m is the propagation coefficient, G_m is the reflection coefficient and $\beta_m = \sqrt{k^2\varepsilon_m - \xi_{11}^2}$. Applying the same boundary conditions between the waveguides we obtain the corresponding 4x4 linear system $AX = B$, where

$$A = \begin{bmatrix} 1 & 1 & -1 & 0 \\ \beta_m & -\beta_m & \beta & 0 \\ e^{-j\beta_m d} & e^{j\beta_m d} & 0 & -e^{-j\beta d} \\ \beta_m e^{-j\beta_m d} & -\beta_m e^{j\beta_m d} & 0 & -\beta e^{-j\beta d} \end{bmatrix}, \quad X = \begin{bmatrix} C_m \\ G_m \\ G \\ D \end{bmatrix}, \quad B = \begin{bmatrix} 1 \\ \beta \\ 0 \\ 0 \end{bmatrix}.$$

We solve numerically this system for various dielectric profiles ε_m obtaining values for C_m, G_m which are in extremely close agreement with our Frobenius approximation. This can be seen, in a wide range of frequencies, in Figures 2 and 3.

Figure 2 to be placed here.

Figure 3 to be placed here.

Case 2: $\varepsilon_r(z) = a + bz$. In the case of linear inhomogeneity eq.(10) becomes

$$Z_r'' + [k^2(a+bz) - \xi^2] \cdot Z_r = 0 \Leftrightarrow Z_r'' + (k^2 a - \xi^2 + k^2 bz) \cdot Z_r = 0 \Leftrightarrow Z_r'' + (A + Bz) \cdot Z_r = 0,$$

where $A = k^2 a - \xi^2$ and $B = k^2 b$. Applying the change of independent variable: $n(z) = -B^{1/3} \cdot (z + \frac{A}{B})$, we obtain

$$\ddot{Z}_r = n Z_r \tag{29}$$

where $\ddot{Z}_r$ denotes the second derivative with respect to n. The general solution of (29) is a linear combination of the *Airy's* functions $Ai(n)$, $Bi(n)$, of the first and second kind, respectively. Consequently, the z-dependent parts of the field components have the expression

$$Z_r(z) = a_1 Ai(n(z)) + a_2 Bi(n(z)) \,, \quad Z_\phi(z) = q Z_r(z) \,,$$

where a_1, a_2 are arbitrary coefficients. Therefore, the field inside the medium waveguide can be explicitly written as

$$E_r(r,\, \phi,\, z) = \frac{j\omega\mu_0}{\xi_{11}^2} \cdot C \frac{J_1(\xi_{11} r)}{r} \sin(\phi)(a_1 Ai(n(z)) + a_2 Bi(n(z)))$$

$$E_\phi(r,\, \phi,\, z) = \frac{j\omega\mu_0}{\xi_{11}} C J_1'(\xi_{11} r) \cos(\phi)(a_1 Ai(n(z)) + a_2 Bi(n(z))) \,.$$

Applying the same boundary conditions at the points $z = 0 \Leftrightarrow n_0 \equiv n(0) = -\frac{A}{B^{2/3}}$ and $z = d \Leftrightarrow n_d \equiv$

$n(d) = -B^{-1/3} \cdot (d + \frac{A}{B})$ we obtain the corresponding 4x4 linear system $AX = B$, where

$$A = \begin{bmatrix} Ai(n_0) & Bi(n_0) & -1 & 0 \\ -B^{1/3}Ai'(n_0) & -B^{1/3}Bi'(n_0) & -j\beta & 0 \\ Ai(n_d) & Bi(n_d) & 0 & -e^{-j\beta d} \\ -B^{1/3}Ai'(n_d) & -B^{1/3}Bi'(n_d) & 0 & j\beta e^{-j\beta d} \end{bmatrix}, \quad X = \begin{bmatrix} a_1 \\ a_2 \\ G \\ D \end{bmatrix}, \quad B = \begin{bmatrix} 1 \\ -j\beta \\ 0 \\ 0 \end{bmatrix}.$$

We solve this system numerically for various linear profiles $\varepsilon_r(z) = a + bz$ and we obtain values for G and D which are in extremely close agreement with our Frobenius approximation, as can be seen in Figures 4 and 5

Figure 4 to be placed here.

Figure 5 to be placed here.

Hence our solutions (obtained using Frobenius method) are in agreement with independently obtained and well known solutions for the two dielectric profiles discussed above.

4.4 Cut-off frequencies

As is well known, in the case of wave propagation through a homogeneous dielectric material, the cut–off frequency for mode TE_{nm} is determined by the equation $\mathbf{f}_{c,nm} = \frac{\xi_{nm}}{2\pi\sqrt{m_0 e_0 \varepsilon_c}}$, $n, m = 1, 2, \ldots$. Namely, for excitation frequencies below $\mathbf{f}_{c,nm}$, the value of the transmission coefficient is very near to zero.

The concept of a cut-off frequency can be extended for the case of inhomogeneous dielectric materials. Namely, it can be expected that for any particular mode TE_{nm}, there will be a frequency $\mathbf{f}_{c,nm}$ with the following property: when the excitation frequency f is below $\mathbf{f}_{c,nm}$, the value of the transmission coefficient is very near to zero.

We have observed by numerical experimentation that our solution has this behavior for the TE_{11} mode. Hence we now proceed to give a precise definition of the cut-off frequency $\mathbf{f}_{c,11}$ in an inhomogeneous dielectric material and to compute the dependence of $\mathbf{f}_{c,11}$ on the dielectric profile.

We define $\mathbf{f}_{c,11}$ to be the frequency at which the transmisison coefficient becomes, for the first time, 0.05. We find that a very good approximation for $\mathbf{f}_{c,11}$, can be given by utilizing a formula analogous to the one applying in the case of constant dielectric permittivity. Namely, we find that

$$\overline{\mathbf{f}}_{c,11} = \frac{\xi_{11}}{2\pi\sqrt{m_0 e_0 \overline{\varepsilon}}}$$

(where $\overline{\varepsilon} = \frac{1}{d}\int_0^d \varepsilon_r(z)dz$ is the mean value of the dielectric profile) is a very good approximation to $\mathbf{f}_{c,11}$, which can be computed experimentally according to the above definition. In Table 1 we give a comparison of $\mathbf{f}_{c,11}$ and $\overline{\mathbf{f}}_{c,11}$ for some representative dielectric profiles.

Table 1

$\varepsilon_r(z)$	$\overline{\varepsilon}$	$\overline{\mathbf{f}}_{c,11}$	$\mathbf{f}_{c,11}$	Rel. Error %
$2.5 + 5.47z$	3.047	1.6774	1.635	2.5933
$2.95 + 5.47z$	3.497	1.5658	1.525	2.6754
$3.12 + 5.47z$	5.647	1.2322	1.185	3.9831
$3.55 + 10.47z$	4.597	1.3657	1.32	3.4621
$4.25 - 13.47z$	2.903	1.7185	1.652	4.0254
$5.13 - 13.47z$	3.783	1.5054	1.45	3.8207
$5.45 - 13.47z$	4.103	1.4455	1.38	4.7464
$2.15 + 25.47z - 120.24z^2$	3.0938	1.6647	1.585	5.0284
$2.75 + 5.47z - 50.24z^2$	2.6271	1.8065	1.75	3.2286
$2.95 + 25.47z - 120.24z^2$	3.8938	1.4839	1.424	4.2065
$3.15 + 10.47z - 50.24z^2$	3.5271	1.5591	1.505	3.5947
$4 - 13.47z + 50.24z^2$	3.3229	1.6063	1.575	1.9873
$5.3 - 13.47z + 50.24z^2$	4.6229	1.3618	1.325	2.7774
$5.9 - 13.47z + 50.24z^2$	5.2229	1.2812	1.24	3.3226
$3.25 - 13.47z + 279.24z^2 - 946.92z^3$	3.7324	1.5156	1.455	4.1649
$3.75 - 13.47z + 279.24z^2 - 946.92z^3$	4.2324	1.4233	1.37	3.8905
$4.25 - 13.47z + 200.24z^2 - 946.92z^3$	3.679	1.5266	1.47	3.8503
$4.75 - 13.47z + 200.24z^2 - 946.92z^3$	4.179	1.4323	1.375	4.1673
$5.4 + 10.47z - 250.24z^2 + 746.92z^3$	4.6043	1.3646	1.308	4.3272
$6.25 + 10.47z - 250.24z^2 + 746.92z^3$	5.4543	1.2537	1.19	5.3529
$7.2 + 10.47z - 250.24z^2 + 746.92z^3$	6.4043	1.157	1.1	5.1818

5 Solving the Inverse Problem: Error Function Minimization

5.1 Formulating the Error Function

We now formulate the estimation of the unknown $\boldsymbol{\varepsilon}$ parameters as a minimization problem. Recall that at this point we have obtained concrete expressions $D(\boldsymbol{\varepsilon},\, f,\, a,\, d)$ and $G(\boldsymbol{\varepsilon},\, f,\, a,\, d)$. By "concrete expressions" we mean that substitution of numerical values for the dielectric permittivity parameters $\boldsymbol{\varepsilon}$, for the frequency f, and for the waveguide geometry parameters a, d yields numerical values for D and G. Now, for a specific measurement device a and d will be fixed. We can choose the excitation frequency f; and in fact we can use several different frequencies, call them $f_1,\, f_2,\, \ldots\, ,\, f_K$. Then we can define an *error function*

$$J_1(\boldsymbol{\varepsilon}) = \sum_{k=1}^{K} \left(\|D_k - D(\boldsymbol{\varepsilon},\, f_k,\, a,\, d)\| + \|G_k - G(\boldsymbol{\varepsilon},\, f_k,\, a,\, d)\| \right)$$

where $\|\cdot\|$ denotes the norm of a complex number. D_k, G_k are the transmission and reflection coefficients (easily computed from field *measurements*) corresponding to source frequency f_k, while $D(\boldsymbol{\varepsilon},\, f_k,\, a,\, d)$ and $G(\boldsymbol{\varepsilon},\, f_k,\, a,\, d)$ are the theoretically obtained values of the same quantities. Hence $J_1(\boldsymbol{\varepsilon})$ measures the discrepancy between observed and theoretically predicted quantities, over all excitation frequencies used in the estimation experiment. Estimation consists in determining $\boldsymbol{\varepsilon}$ values which minimize the discrepancy $J_1(\boldsymbol{\varepsilon})$. The globally minimum value would be achieved at some $\widehat{\boldsymbol{\varepsilon}}$ such that $J_1(\widehat{\boldsymbol{\varepsilon}}) = 0$. In such a case, theory and measurement would be in perfect agreement. Of course, such a goal is not realistic, since various factors (polynomial approximation to $\varepsilon(z)$, limited measurement precision etc.) will result in positive values of $J_1(\widehat{\boldsymbol{\varepsilon}})$. Realistically, the best that can be hoped for is a very small value of $J_1(\widehat{\boldsymbol{\varepsilon}})$.

Use of $J_1(\boldsymbol{\varepsilon})$ is based on the assumption that one can measure the real and complex parts of D, G, which is equivalent to measuring both amplitude and phase of D, G. In case measurement of the phase

is either impossible or impractical, an alternative error function can be used, defined as follows

$$J_2(\boldsymbol{\varepsilon}) = \sum_{k=1}^{K} | \, \|D_k\| - \|D(\boldsymbol{\varepsilon},\, f_k,\, a,\, d)\| \, | + | \, \|G_k\| - \|G(\boldsymbol{\varepsilon},\, f_k,\, a,\, d)\| \, |$$

where $|\cdot|$ denotes the absolute value.

5.2 Function Minimization by Genetic Algorithms

We have performed the error function minimization indicated in the previous section by the use of a *genetic algorithm*. Genetic algorithms (G.A.'s) perform global optimization by mimicking the natural selection process; they are extensively used in the solution of electromagnetics problems [12].

We have used the so called "Differential Evolution" (DE) optimization algorithm, which is closely related to genetic ones. This algorithm is described in detail in [13]. Let us give here a brief description.

The algorithm attempts to minimize a function $z(\mathbf{x})$, where $\mathbf{x}$ is the independent variables. In standard genetic algorithm fashion, the DE algorithm works for several iterations, each iteration henceforth called a "generation". Every generation contains a number of "phenotypes", i.e. trial values $\mathbf{x}_1^{old}$, $\mathbf{x}_2^{old}$, ... , $\mathbf{x}_N^{old}$ where N is the "population size". The phenotypes of the next generation, call them, $\mathbf{x}_1^{new}$, $\mathbf{x}_2^{new}$, ... , $\mathbf{x}_N^{new}$ are generated from the previous generation $\mathbf{x}_1^{old}$, $\mathbf{x}_2^{old}$, ... , $\mathbf{x}_N^{old}$ by a rule of the form

$$\mathbf{x}_i^{new} = \mathbf{x}_r^{old} + F \cdot (\mathbf{x}_s^{old} - \mathbf{x}_t^{old}) \quad i = 1, 2, ..., N,$$

where r, s, t are chosen randomly (in such a manner that they are all different) from the set $\{1, 2, ..., N\}$. It can be seen that the parameter F controls the amplification of differential variation. If $z(\mathbf{x}_i^{new}) < z(\mathbf{x}_r^{old})$ then $\mathbf{x}_i^{new}$ replaces $\mathbf{x}_r^{old}$ as a member of the new generation. This process of generating new vectors by combining old ones is similar to reproduction of natural species. In addition, a mechanism

which resembles *mutation* generates a new vector by perturbing the parameters of an old one; this process is controlled by a parameter P, the so called "crossover probability" (a large value of P results in strong mutation).

When applying the above algorithm to a function minimization problem, we must also provide a *stopping criterion*. We use the following: the algorithm terminates (and the currently best vector $\widehat{\mathbf{x}}$ is accepted) if the value of the function becomes less than a prespecified threshold δ; a prespecified maximum number of iterations may also be provided.

6 Numerical Results

We now present experiments of dielectric permittivity reconstruction. These are *simulated experiments*, i.e. they do not involve measurement of an actual physical system. Instead, we postulate a three-waveguide measurement system of the form presented in Section 4.1 with d=20cm, a=3cm and specific $\boldsymbol{\varepsilon}$ and ε_c values. Then we obtain numerical values for the field inside the system by utilizing the analysis presented in Section 4.2. These numerical values are our "virtual measurements". Then, we assume the $\boldsymbol{\varepsilon}$ values to be unknown and we utilize the error function minimization formulation of Section 5 and the inverse problem solution of Section 4 to obtain "good" estimates $\widehat{\boldsymbol{\varepsilon}}$ of the true $\boldsymbol{\varepsilon}$ values (i.e. estimates $\widehat{\boldsymbol{\varepsilon}}$ which yield a near zero value of the error function).

We choose the permittivity ε_c to be $\varepsilon_c = 8$, so that $f_{c,11} = \frac{\xi_{11}}{2\pi\sqrt{m_0 e_0 \varepsilon_c}} = \frac{1.841}{2\pi a\sqrt{m_0 e_0 8}} = 1.0352GHz$ and $f_{c,12} = \frac{\xi_{12}}{2\pi\sqrt{m_0 e_0 \varepsilon_c}} \cong 2.896 f_{c,11} = 2.998GHz$. Hence, in accordance with the remarks in Section 4.4, we expect that, for frequencies in the range $[f_{c,11}\ f_{c,12}]$ only the TE_{11} mode will propagate inside the waveguides.

6.1 Experiment Setup

In our virtual experiments we use four frequency values: $f_1 = 1.7,\ f_2 = 1.8,\ f_3 = 2,\ f_4 = 2.4$ (measured in GHz). As for the genetic algorithm parameters, we have found that the choices listed in Table 2 yield sufficiently accurate parameter estimates.

Table 2

Parameter	**Significance**
$V_{\min}$= [1 -40 -400 -1000]	Lower limits for the parameters.
$V_{\max}$= [7.5 40 400 1000]	Upper limit for the parameters.
N=120	Number of trial vectors per generation.
Iterations=150	Maximum number of generations.
F=0.5	Diff. variation amplification.
P=0.8	Crossover probability.

The $V_{\min}$ and $V_{\max}$ values were chosen so as to ensure that all $\boldsymbol{\varepsilon}$ values of practical interest will be included in the hyperrectangle of the 4-D space which will be searched by the DE algorithm. Finally, our experiments have indicated that $\delta = 10^{-1}$ is a good value for the stopping criterion threshold. In other words, stopping the algorithm when $J_1(\widehat{\boldsymbol{\varepsilon}})$ or $J_2(\widehat{\boldsymbol{\varepsilon}})$ becomes less than 10^{-1} yields accurate estimates of $\boldsymbol{\varepsilon}$. This generally takes place in less than 100 iterations.

In Sections 6.2, 6.3 we present our estimates of the $\boldsymbol{\varepsilon}$ coefficients as obtained using two kinds of data; i.e measurements of (i) only amplitudes of D and G, (ii) amplitudes and phases of D and G.

6.2 Amplitude Measurements

In this case the experimental data are the amplitudes of D and G. The diagrams that follow reproduce the results obtained by the DE algorithm. Namely, Figure 6 presents the minimum value of the error function for every second iteration of the DE algorithm. Figures 7–10 present the evolution of the

$\hat{\varepsilon}_0$, $\hat{\varepsilon}_1$, $\hat{\varepsilon}_2$, $\hat{\varepsilon}_3$ parameter estimates, respectively.

Figure 6 to be placed here.

Figure 7 to be placed here.

Figure 8 to be placed here.

Figure 9 to be placed here.

Figure 10 to be placed here.

With respect to the error function value the final best estimate, after 80 iterations, is

$$\widehat{\boldsymbol{\varepsilon}} = [\hat{\varepsilon}_0\ \hat{\varepsilon}_1\ \hat{\varepsilon}_2\ \hat{\varepsilon}_3] = [3.11\ \ -15.11\ \ 293.31\ \ -988.39]$$

while the true value is

$$\boldsymbol{\varepsilon} = [\varepsilon_0\ \varepsilon_1\ \varepsilon_2\ \varepsilon_3] = [3.05\ \ -13.47\ \ 279.24\ \ -946.92]\,.$$

Let us define the estimate error vector as follows:

$$\Delta\boldsymbol{\varepsilon} = \left[\left|\frac{\varepsilon_0 - \hat{\varepsilon}_0}{\varepsilon_0}\right| \quad \left|\frac{\varepsilon_1 - \hat{\varepsilon}_1}{\varepsilon_1}\right| \quad \left|\frac{\varepsilon_2 - \hat{\varepsilon}_2}{\varepsilon_2}\right| \quad \left|\frac{\varepsilon_3 - \hat{\varepsilon}_3}{\varepsilon_3}\right|\right]\,.$$

Then we have $\Delta\boldsymbol{\varepsilon} = [0.02\ \ 0.12\ 0.05\ \ 0.04]$. The estimates obtained gives a very good approximation of the true dielectric profile, as can be seen in Figure 11.

Figure 11 to be placed here.

6.3 Amplitude & Phase Parts Measurement

In this case the experimental data are the amplitudes and the phases of D and G. Similarly, the diagrams below reproduce the results obtained by the DE algorithm. Figure 12 presents the minimum value of the error function for every second iteration of the DE algorithm and Figures 13–16 present the evolution of the best $\hat{\varepsilon}_0$, $\hat{\varepsilon}_1$, $\hat{\varepsilon}_2$, $\hat{\varepsilon}_3$ parameter estimates, respectively.

Figure 12 to be placed here.

Figure 13 to be placed here.

Figure 14 to be placed here.

Figure 15 to be placed here.

Figure 16 to be placed here.

The final best (with respect to the error function value) estimate, after 93 iterations, is

$$\widehat{\boldsymbol{\varepsilon}} = [\hat{\varepsilon}_0\ \hat{\varepsilon}_1\ \hat{\varepsilon}_2\ \hat{\varepsilon}_3] = [3.02\ \ -13.67\ \ 281.7\ \ -933.21]$$

while the true value is

$$\boldsymbol{\varepsilon} = [\varepsilon_0\ \varepsilon_1\ \varepsilon_2\ \varepsilon_3] = [3.05\ \ -13.47\ \ 279.24\ \ -946.92]\,.$$

Now, the error vector becomes $\Delta\boldsymbol{\varepsilon}$ =[0.01 0.015 0.09 0.015]. Also, in this case our estimation gives a very good approximation of the true dielectric profile, too. This can be seen in Figure 17.

Figure 17 to be placed here.

7 Conclusions

In this paper we have solved the problem of electromagnetic wave propagation in a waveguide completely filled with a dielectric material inhomogeneous in the longitudinal direction. We have first solved the direct problem representing the waves in the inhomogeneous medium based on the Frobenius method. We also noticed that a good approximation of the cut-off frequency of the propagating modes is given by utilizing the mean value of the dielectric profile. Then we have developed a computational procedure for solving the inverse problem. This procedure, making use of error function minimization by a genetic algorithm, was applied to the estimation of unknown dielectric permittivity profiles and yielded very accurate results.

References

[1] Tyras G., *Radiation and Propagation of Electromagnetic Waves.* New York, Academic Press, 1969.

[2] Weng Cho Chew, *Waves and Fields in Inhomogeneous Media*, IEEE Press, 1995.

[3] Tantot O., Chatard-Moulin M., Guillon P., *Measurement of complex permittivity and permeability and thickness of multilayered medium by an open-ended waveguide method*, IEEE Trans. Instr. & Measurement, vol.46, pp.519-522, 1997.

[4] Gevorkian E. A., *On the theory of propagation of electromagnetic waves in a waveguide with a multiperiodically modulated dielectric filling*, Phys. A: Statistical and Theoritical Physics, vol. 241, pp. 236-239, 1997.

[5] Rafizadeh D., Seng-Tiong Ho, *Numerical analysis of vectorial wave propagation in waveguides with arbitrary refractive index profiles*, Optics Communications, 1997, Vol. 141, pp. 17-20.

[6] Potter D., *Computational Physics.* New York: Wiley Interscience, 1973.

[7] Christopoylos C., *The Transmission-Line Modeling Method:TLM*, IEEE Press, 1995.

[8] Mathey P., Jullien P., *Numerical analysis of a WKB inverse method in view of index profile reconstruction in diffused waveguides*, Optics Communications, 1996, Vol. 122, pp. 127-134.

[9] Birkhoff, G., Rota, G. *Ordinary Differential Equations*. Ginn and Company, 1962.

[10] Hille, E. *Ordinary Differential Equations in the Complex Plane*. Dover, 1976.

[11] Balanis K., *Advanced Engineering Electromagnetics*, J.Willey & Sons, N.Y., 1998.

[12] Weile D.S., Miclielssen E., *Genetic Algorithm optimization applied to electromagnetics: A review,* IEEE Trans. Antennas & Propag., vol.45, pp.343-353, March 1997.

[13] Storn R., Prise K., *Differential Evolution - a Simple and Efficient Heuristic for Global Optimization over Continuous Spaces*, Kluwer Academic Publishers, 1997, Vol.11, pp. 341-359.

List of Captions

Figure 1: The measurement device.

Figure 2: Error of the absolute value of D as a function of frequency, for constant dielectric profile ϵ_m=3. (Computed as the relative absolute difference between our solution and the one involving trigonometric functions)

Figure 3: Error of the absolute value of G as a function of frequency, for constant dielectric profile ϵ_m=3. (Computed as the relative absolute difference between our solution and the one involving trigonometric functions.)

Figure 4: Error of the absolute value of D as a function of f, for the linearly varying dielectric $\epsilon_r(z) = 3 + 20z$. (Computed as the relative difference between our solution and the one involving Airy's functions.)

Figure 5: Error of the absolute value of G as a function of f, for linearly varying dielectric. $\epsilon_r(z) = 3 + 20z$. (Computed as the relative difference between our solution and the one involving Airy's functions.)

Figure 6: Error function values as a function of G.A.'s iterations.

Figure 7: Evolution of the estimated ϵ_0 coefficient as a function of G.A.'s iterations.

Figure 8: Evolution of the estimated ϵ_1 coefficient as a function of G.A.'s iterations.

Figure 9: Evolution of the estimated ϵ_2 coefficient as a function of G.A.'s iterations.

Figure 10: Evolution of the estimated ϵ_3 coefficient as a function of G.A.'s iterations.

Figure 11: Comparative diagram between our estimated-guess dielectric profile and the real one along the medium waveguide.

Figure 12: Error function values as a function of G.A.'s iterations

Figure 13: Evolution of the estimated ϵ_0 coefficient as a function of G.A.'s iterations

Figure 14: Evolution of the estimated ϵ_1 coefficient as a function of G.A.'s iterations.

Figure 15: Evolution of the estimated ϵ_2 coefficient as a function of G.A.'s iterations.

Figure 16: Evolution of the estimated ϵ_3 coefficient as a function of G.A.'s iterations.

Figure 17: Comparation diagram between our estimated-guess dielectric profile and the real one along the medium waveguide.

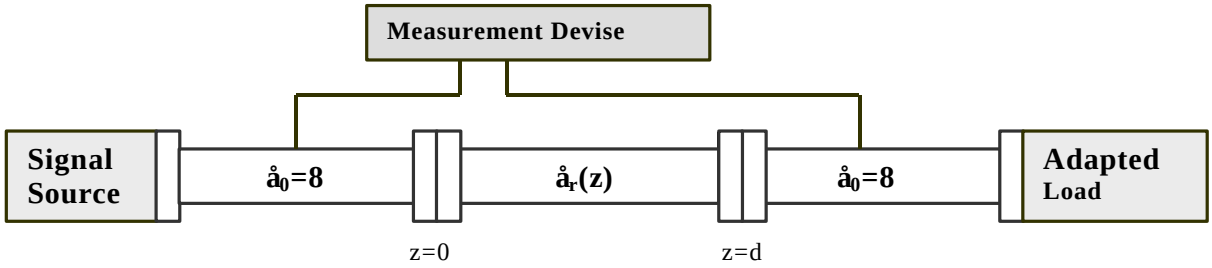

Figure 1: The measurement device.

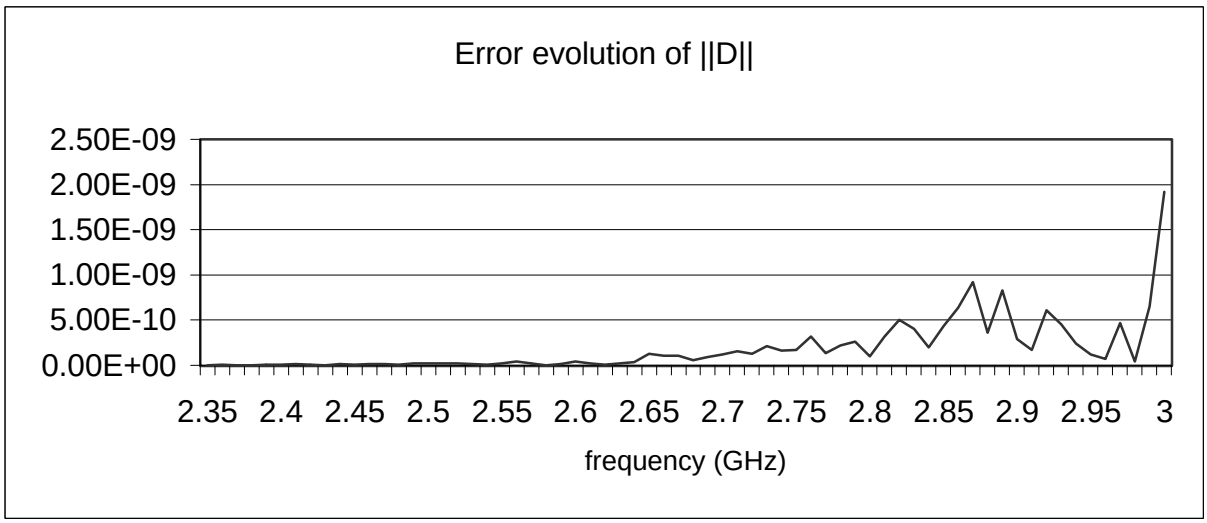

Figure 2: Error of the absolute value of D as a function of frequency, for constant dielectric profile åm=3. (Computed as the relative absolute difference between our solution and the one involving trigonometric functions)

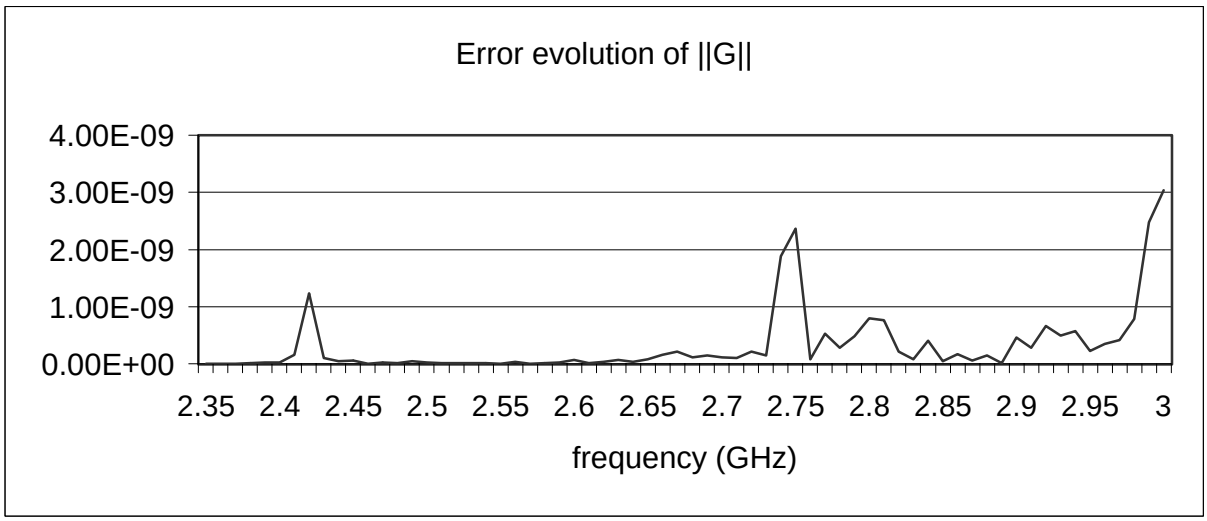

Figure 3: Error of the absolute value of G as a function of frequency, for constant dielectric profile åm=3. (Computed as the relative absolute difference between our solution and the one involving trigonometric functions)

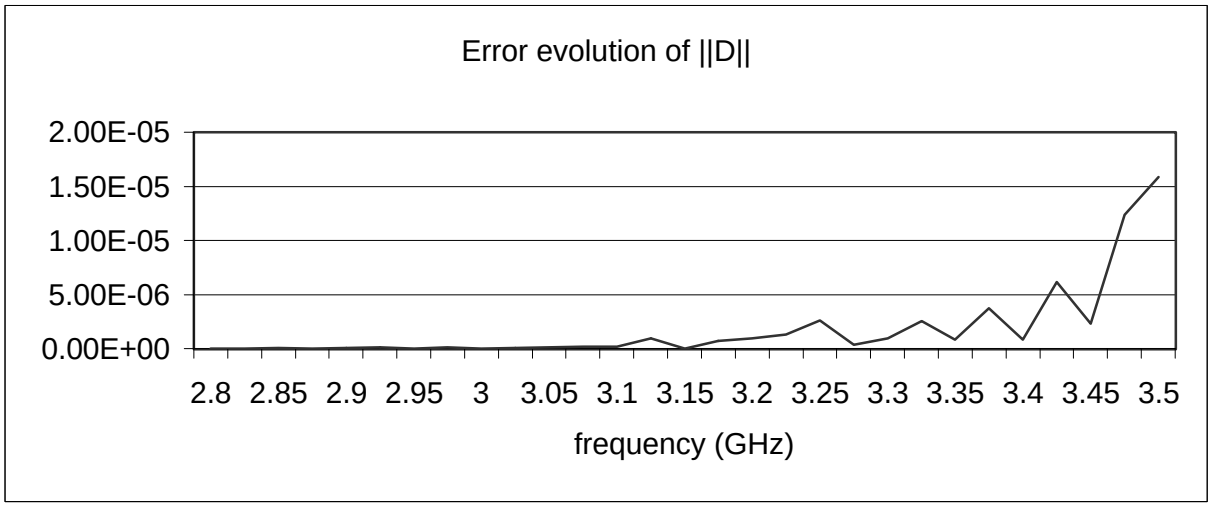

Figure 4: Error of the absolute value of D as a function of f, for the linearly varying dielectric er(z)=3+20z. (Computed as the relative difference between our solution and the one involving Airy's functions.)

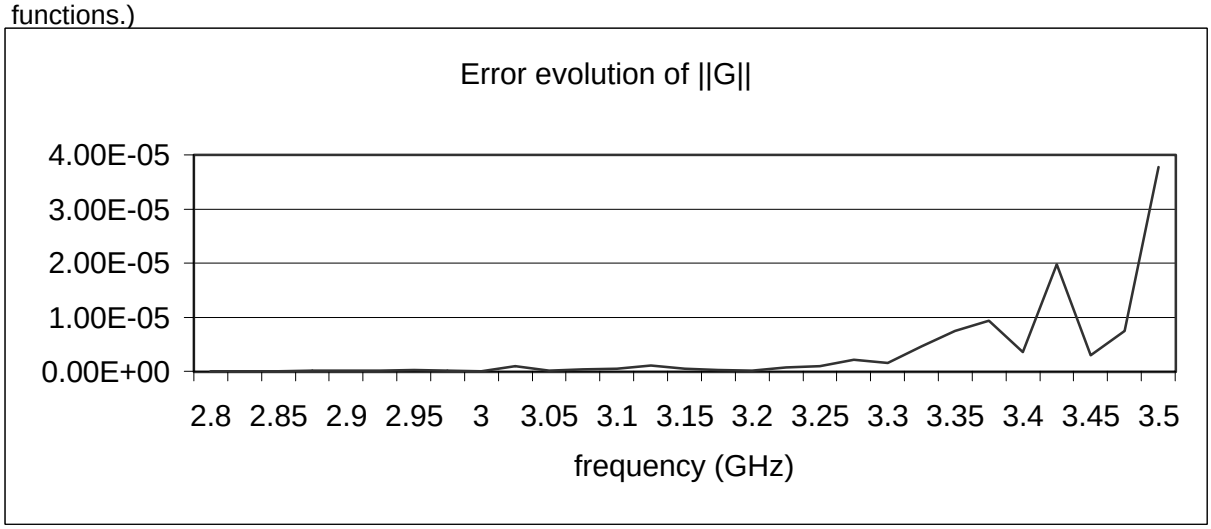

Figure 5: Error of the absolute value of G as a function of f, for linearly varying dielectric. er(z)=3+20z. (Computed as the relative difference between our solution and the one involving Airy's functions.)

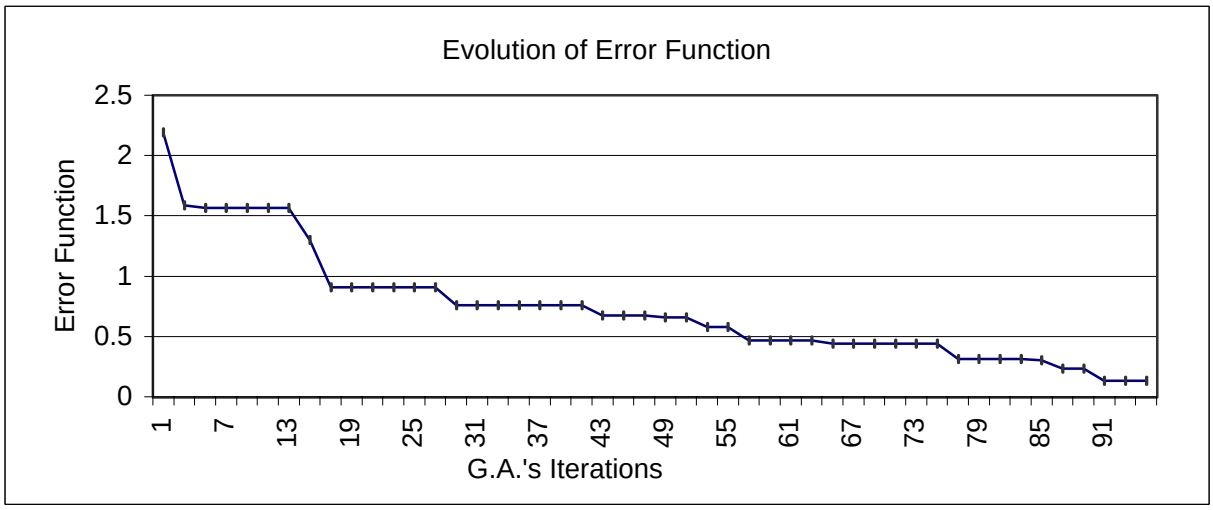

Figure 6: Error function values as a function of G.A.'s iterations

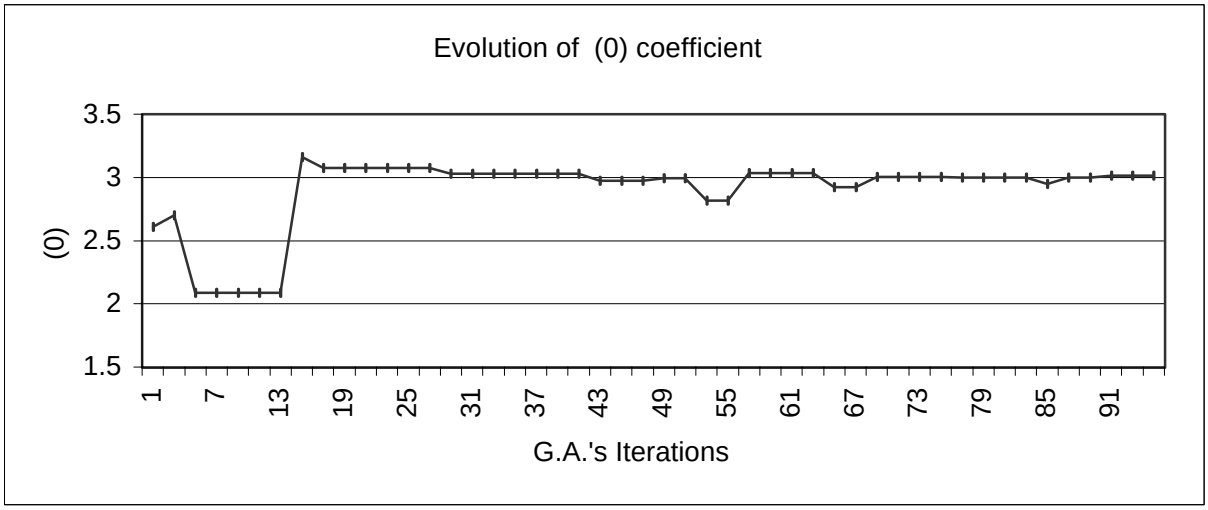

Figure 7: Evolution of the estimated (0) coefficient as a function of G.A.'s iterations

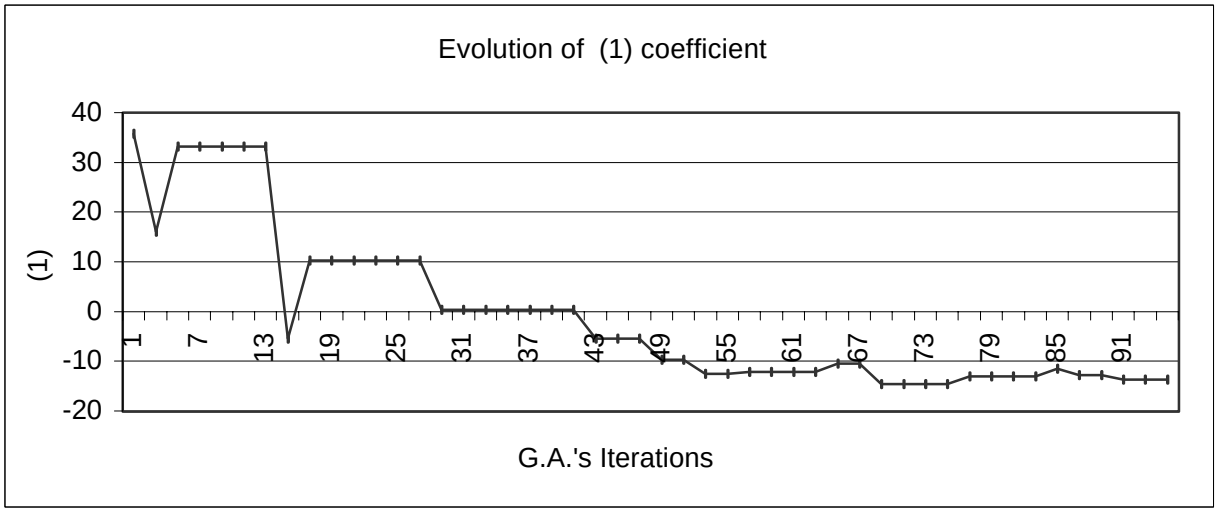

Figure 8: Evolution of the estimated (1) coefficient as a function of G.A.'s iterations

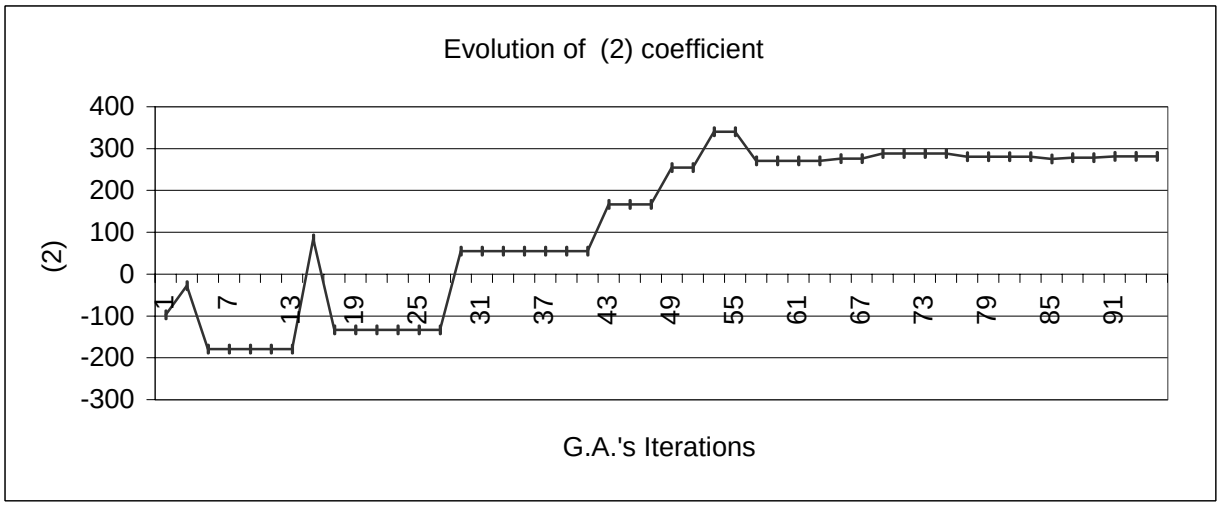

Figure 9: Evolution of the estimated (2) coefficient as a function of G.A.'s iterations

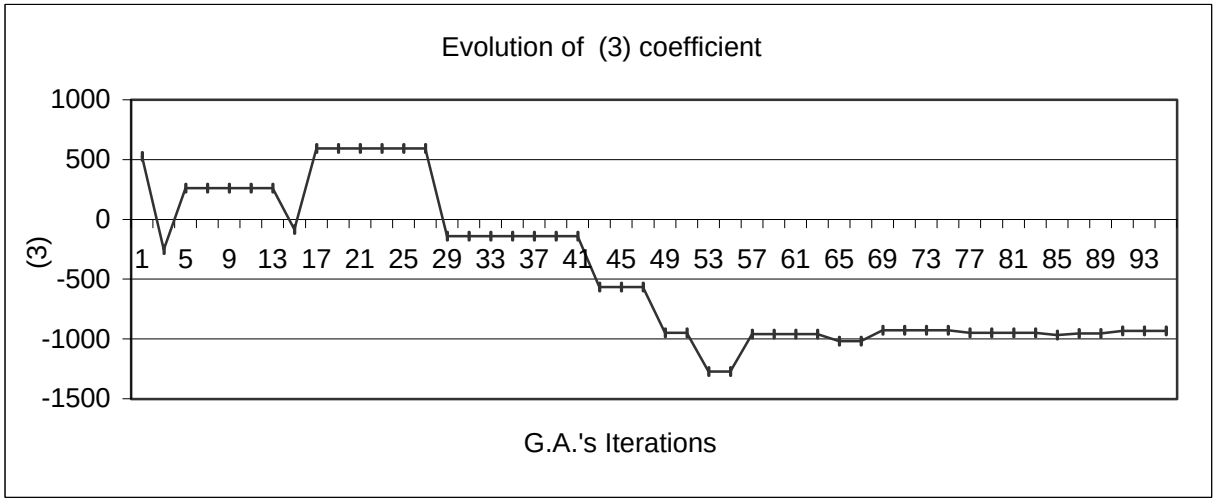

Figure 10: Evolution of the estimated (3) coefficient as a function of G.A.'s iterations

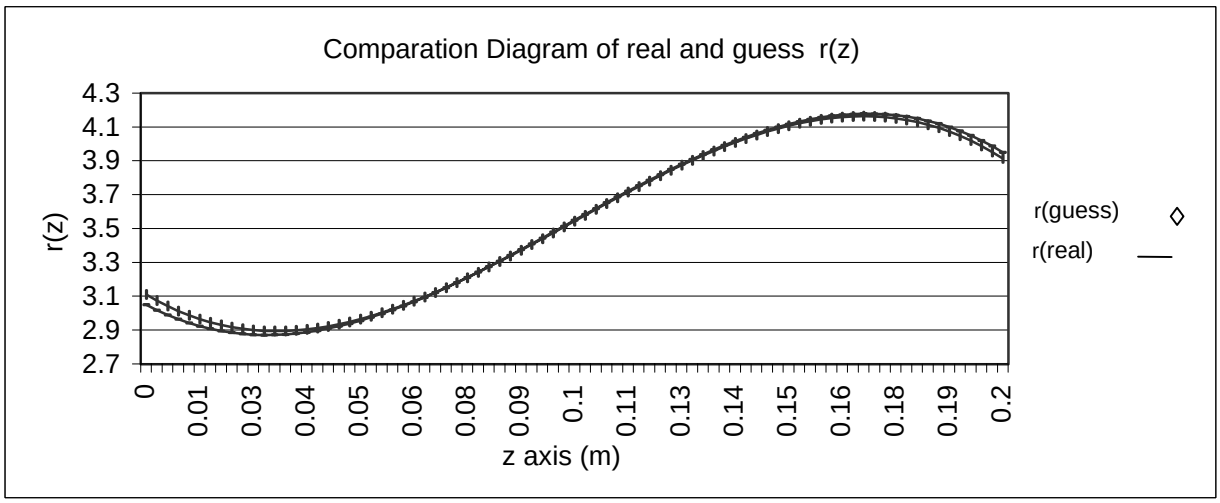

Figure 11: Comparative diagram between our estimated-guess dielectric profile and the real one along the medium waveguide.

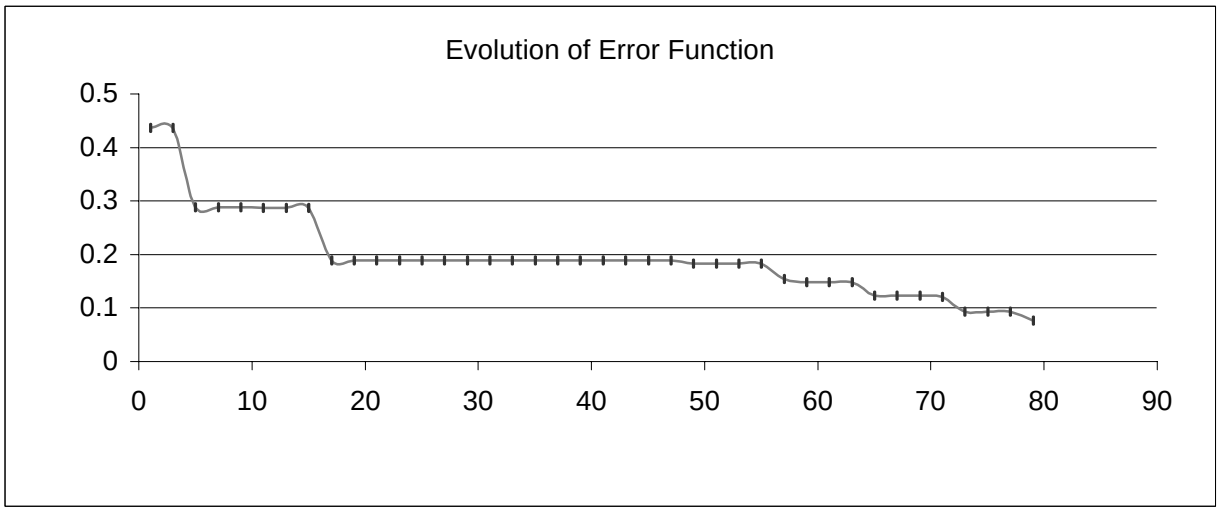

Figure 12: Error function values as a function of G.A.'s iterations

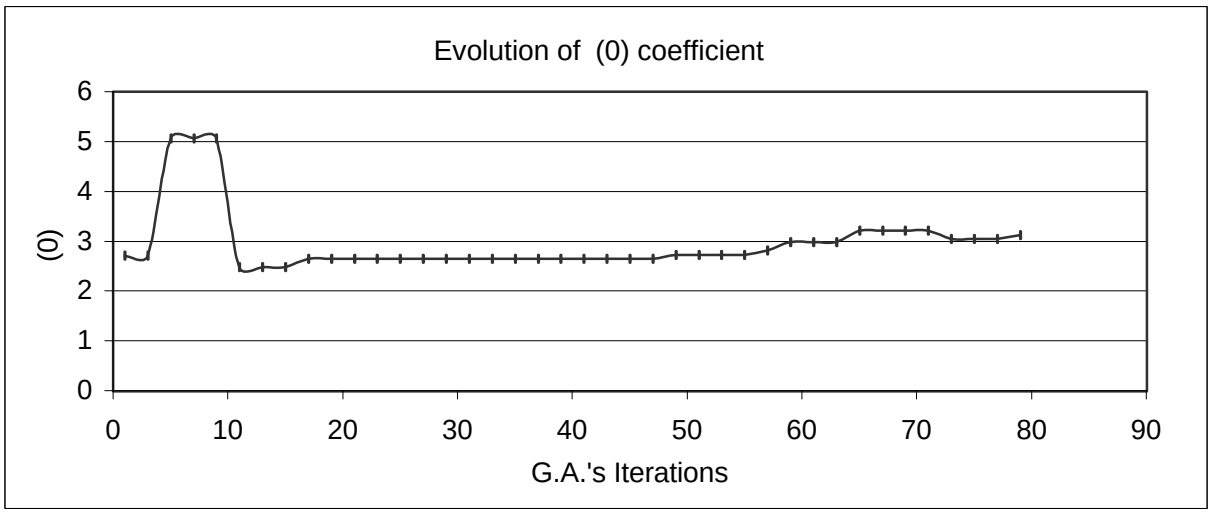

Figure 13: Evolution of the estimated (0) coefficient as a function of G.A.'s iterations

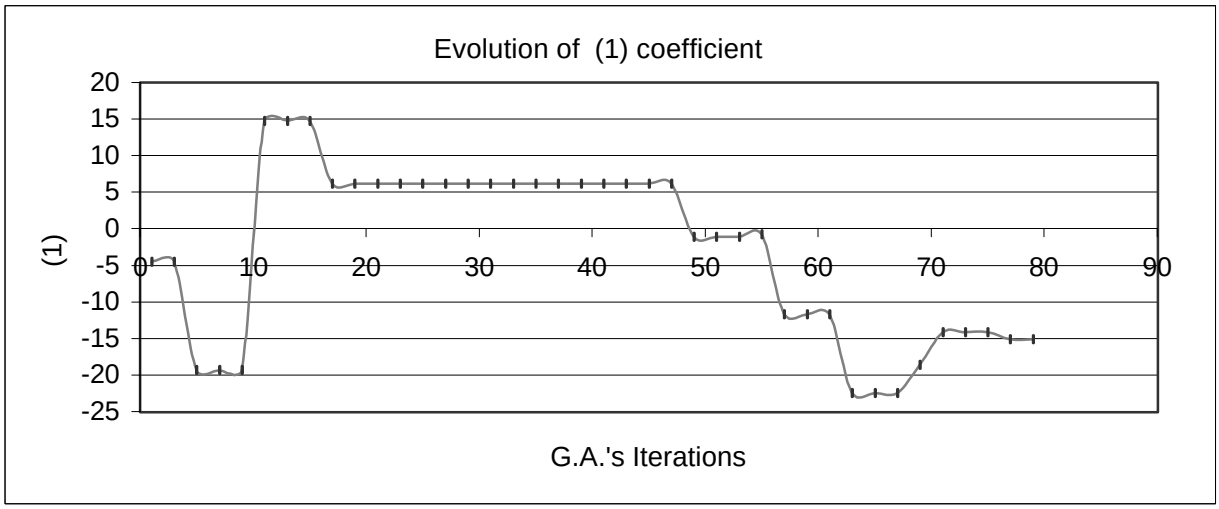

Figure 14: Evolution of the estimated (1) coefficient as a function of G.A.'s iterations

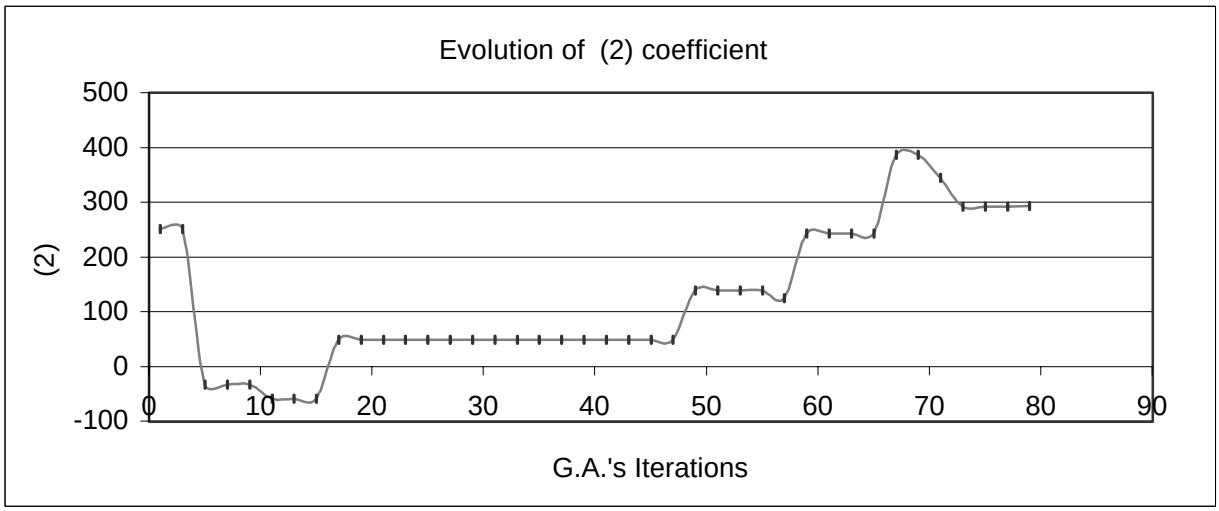

Figure 15: Evolution of the estimated (2) coefficient as a function of G.A.'s iterations

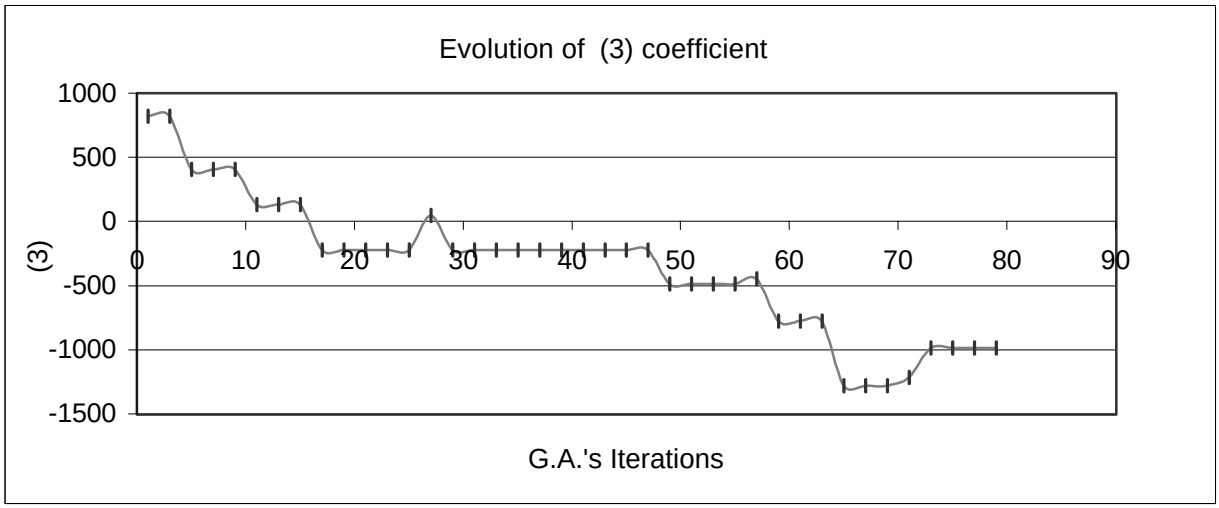

Figure 16: Evolution of the estimated (3) coefficient as a function of G.A.'s iterations

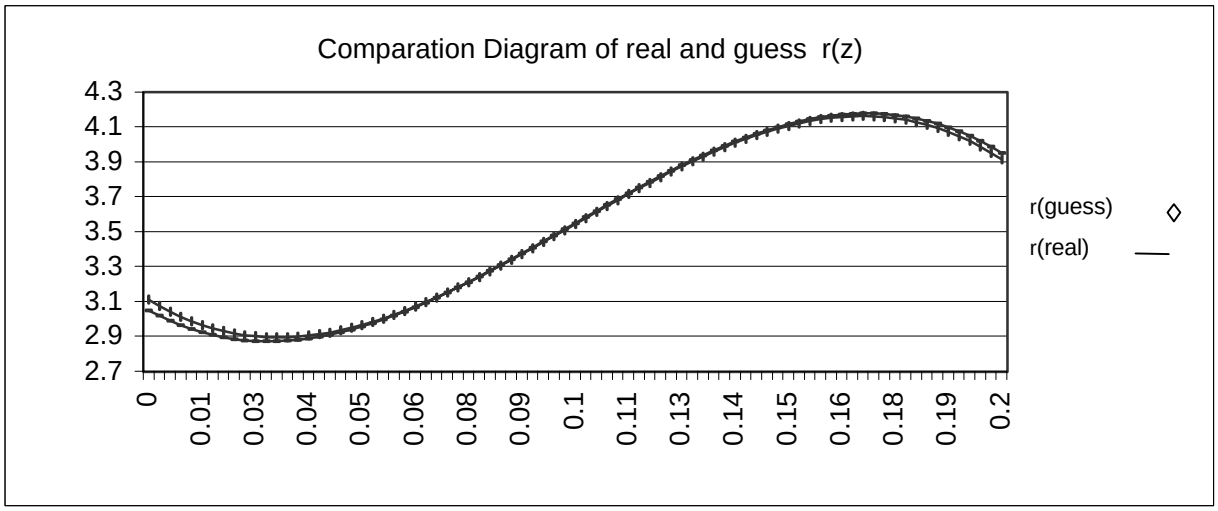

Figure 17: Comparation diagram between our estimated-guess dielectric profile and the real one along the medium waveguide.